Jurnal Tribologi 39 (2023) 69-83

MYTRIBOS Malaysian Tribology Society

Jurnal Tribologi

Website : jurnaltribologi.mytribos.org e-issn: 2289-7232

Tribological properties and thermal behaviour of Ti_3C_2 MXene as anti-friction and heat transfer additive in outboard engine oil

Mariyam Jameelah Ghazali [1], Haizum Aimi Zaharin[1*], Mohammad Khalid [2,3], Thachnatharen Nagarajan [4]

[1]Department of Mechanical and Manufacturing Engineering, Faculty of Engineering and Built Environment, Universiti Kebangsaan Malaysia, MALAYSIA.
[2] Sunway Centre for Electrochemical Energy and Sustainable Technology (SCEEST), School of Engineering and Technology, Sunway University, No. 5, Jalan Universiti, Selangor Darul Ehsan, 47500, Petaling Jaya, Bandar Sunway, MALAYSIA.
[3] Sunway Materials Smart Science and Engineering (SMS2E) Research Cluster, Sunway University, No. 5, Jalan Universiti, Bandar Sunway, Petaling Jaya, Selangor 47500, MALAYSIA.
[4] Faculty of Defence Science and Technology, National Defence University of Malaysia, Kuala Lumpur, MALAYSIA.
[*]Corresponding author: haizumaimi262@gmail.com

KEYWORDS

Ti_3C_2 MXene
Nanoparticle
COF
Wear
Thermal conductivity

ABSTRACT

Two-dimensional materials added and distributed in lubricating oil have been shown to improve the tribological properties of the oil. In this work, 2D Ti_3C_2 MXene nanoparticles, synthesized via the advanced microwave-assisted hydrothermal platform, were characterized using FESEM, EDX, XRD, and FTIR to study their morphology, chemical composition and the interaction between their functional groups. The as-prepared Ti_3C_2 MXene nanoparticles with nanoparticles size around 12 nm were introduced as an additive to outboard engine oil to reduce the tribological effect between contact surfaces. The findings demonstrate that adding 0.01 wt.% of Ti_3C_2 MXene reduced the friction by 5.8% and wear by 6.0%, owing to the possibility for interlaminar shear of Ti_3C_2 MXene nanosheets. At the same time, the thermal conductivity increased by > 50% after 70°C when 0.01 wt.% of Ti_3C_2 MXene was added to outboard engine oil.

Received 22 August 2023; received in revised form 8 September 2023; accepted 6 November 2023.
To cite this article: Zaharin et al. (2023). Tribological properties and thermal behaviour of Ti3C2 MXene as anti-friction and heat transfer additive in outboard engine oil. Jurnal Tribologi 39, pp.69-83.

1.0 INTRODUCTION

In response to the rapid growth of nanotechnology, researchers have turned their attention to utilizing nanomaterials for improving traditional lubricants and optimizing engine performance. Associating nanoparticles, particularly at the nanoscale, into outboard engine oil holds great promise for mitigating marine transportation problems (Rasheed et al., 2020; Zaharin et al., 2022; Zaharin et al., 2023). Nanolubricants, engineered at the nanoscale, have unique properties that reduce wear and friction between engine components, improving mechanical efficiency, fuel economy, and pollution (Ji et al., 2020; Rosenkranz et al., 2020). Additionally, nanolubricants exhibit superior thermal stability, effectively dissipating heat and maintaining optimal engine operating temperatures (Al-Janabi et al., 2021; Masjuki et al., 2014; Nagarajan et al., 2022; Yang et al., 2019). Materials at the nanoscale, which generally ranges from 1 to 100 nanometers, may be purposefully manipulated and controlled with great precision through nanotechnology. This size allows materials to display distinctive characteristics and behaviours different from their bulk equivalents, creating new opportunities for improving lubricants in various applications. (Anasori et al., 2017; Gupta et al., 2020; Rosenkranz et al., 2019; Shahdeo et al., 2020; Ying et al., 2015; Rahman et al., 2023). Furthermore, integrating nanoparticles into engine oil offers significant advantages, including reducing friction by forming protective coatings that minimize direct metal-to-metal contact, thereby reducing mechanical degradation and abrasion (Manu et al., 2021; Rosenkranz et al., 2023; Zaharin et al., 2023). Additionally, the thermal conductivity of these nanoparticles may be improved, enabling effective cooling and decreasing temperature during operation, which is beneficial for engines running in challenging marine circumstances.

Recent studies suggest that adding 2D MXene nanoparticles into outboard engine oils shows promise in tackling tribological issues (Markandan et al., 2023; Rosenkranz et al., 2023; Zaharin 2023). MXenes are layered materials consisting of transition metal carbides, nitrides, or carbonitrides. Ti_3C_2 MXene, in particular, has gained considerable attention attributed to its extraordinary properties (Naguib et al., 2013; Verger et al., 2019). Ti_3C_2 MXene nanoparticles are an intriguing choice for improving engine fluid lubrication and lowering friction because of their characteristics. Ti_3C_2 MXene nanolubricant forms a protective layer on engine surfaces that reduces wear and friction between moving components. Ti_3C_2 MXene's unique 2D structure provides high adherence to surface flaws, improving lubrication and lowering the chance of surface damage. Ti_3C_2 MXene has excellent anti-wear properties and strong load-bearing capacity that can further minimize frictional losses and increase fuel efficiency.

Although Ti_3C_2 MXene offers exceptional properties and potential benefits as a lubricant additive, assessing its toxicity is a critical aspect that requires thorough investigation before its incorporation into lubricants. Several studies have examined the potential toxicity of Ti_3C_2 MXene, primarily focusing on its impact on human health and the environment. A study conducted by Pan et al. (Pan et al., 2020) evaluated the cytotoxicity of Ti_3C_2 MXene on human cell lines and concluded that at low concentrations, Ti_3C_2 MXene exhibited minimal cytotoxic effects. The authors attributed this to the material's limited cellular uptake and biocompatibility. Similarly, Nasrallah et al. (Nasrallah et al., 2018) investigated the severe toxicity of Ti_3C_2 MXene nanoparticles in aquatic organisms and observed negligible adverse effects at environmentally relevant concentrations. Incorporating minute quantities of Ti_3C_2 MXene into lubricants can enhance their tribological and thermal properties, thereby improving engine performance and efficiency. Several studies have explored the effects of incorporating nanomaterials, including Ti_3C_2 MXene, into lubricating oils (Cai et al., 2022; Y. Liu, 2016; Zaharin et al., 2023), the addition of Ti_3C_2 MXene nanoparticles to lubricating oil was shown to reduce friction and wear between

engine components, leading to improved engine efficiency and extended component lifespan. Additionally, the thermal conductivity enhancement of lubricating oils through the dispersion of Ti_3C_2 MXene, aids in effective heat dissipation and preventing excessive engine overheating (Anasori et al., 2017; Markandan et al., 2023; Zaharin et al., 2023).

The primary objective of this research is to conduct a comprehensive investigation to gain a profound understanding of the enhancements achieved by incorporating Ti_3C_2 MXene into base oil. The study thoroughly examines several pivotal characteristics, including the coefficient of friction (COF), average wear scar diameter (WSD), and thermal conductivity. Through these analyses, the overarching aim is to thoroughly comprehend the implications arising from introducing Ti_3C_2 MXene into engine oil. This exploration may lead to the development of entirely innovative and high-performance lubricants. The outcomes derived from this study are expected to yield critical insights into the augmentation of engine oil performance facilitated by Ti_3C_2 MXene additives. This research holds significant promise in addressing tribological challenges and surmounting issues associated with effective heat dissipation in outboard engines.

2.0 MATERIALS AND EXPERIMENTAL PROCEDURE

2.1 Materials

The preparation of MXene powder involved the utilization of various materials. Specifically, Xiamen Tob New Energy Technology Co., Ltd, located in China, procured titanium aluminium carbide (Ti_3AlC_2) in a 400-mesh form with a purity level of 99.9%. Additionally, hydrochloric acid (HCl) with a concentration of 37% v/v and lithium fluoride (LiF) in a 300-mesh form were sourced from Sigma Aldrich, a reputable supplier based in Malaysia. Furthermore, ethanol of 96% purity was also acquired from Sigma Aldrich, Malaysia. In the context of this study, a lubricant oil compatible with TC-W requirements as stipulated by the National Marine Manufacturers Association (NMMA) for outboard engines was employed. It is noteworthy that no supplementary purification procedures were undertaken, as all the chemical reagents used in this research were of analytical-grade quality.

2.2 Synthesis of 2D Ti_3C_2 MXene

The synthesis of Ti_3C_2 MXene was conducted utilizing an advanced microwave-assisted hydrothermal synthesis apparatus, specifically the Milestone FlexiWAVE system from Italy. During the synthesis procedure, hydrofluoric acid (HF) was generated in-situ by combining lithium fluoride (LiF) and concentrated hydrochloric acid (HCl). To mitigate the risk of potentially hazardous exothermic reactions, a methodical approach was employed. Initially, 2.5 M LiF was dissolved in 10 mL of 6 M concentrated HCl within a Teflon tube. Subsequently, 0.5 g of MAX phase material was incrementally introduced into the LiF/HCl solution. Following 30 minutes of magnetic stirring, the mixture underwent an additional 30 minutes of sonication. The resultant solution was subsequently subjected to an advanced hydrothermal system equipped with microwave support, operating at a temperature of 30 °C for a duration of 10 minutes. Figure 1 in the documentation illustrates the schematic representation of the advanced microwave-hydrothermal synthesis process employed for Ti_3C_2 MXene production. Subsequent to the synthesis reaction, the acidic mixture underwent thorough cleaning utilizing ethanol and deionized water. To separate the solid components, centrifugation was carried out at 5,000 revolutions per minute for a period of 5 minutes, employing a Sartorius centrifuge from Germany.

This washing procedure was reiterated until a stable colloidal suspension of MXene was obtained. The final MXene solution achieved through this process was deemed to be pure, devoid of the aluminum layer and any associated by-products. It is important to note that the methodology employed in this study was adapted from prior research conducted by our team(Numan et al., 2022; Zaharin et al., 2023). Figure 1 illustrates the overall process involved in synthesizing Ti_3C_2 MXene nanoparticles.

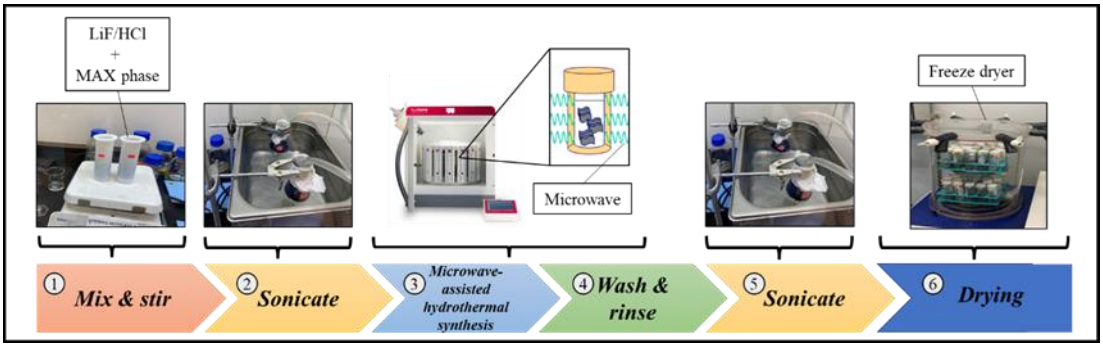

Figure 1: Schematic diagram of Ti_3C_2 MXene nanoparticles preparation via advanced microwave synthesis.

2.3 Characterization of 2D Ti_3C_2 MXene Nanoparticles

The investigation of the phase structure and crystallinity of the synthesized Ti_3C_2 MXene nanoparticles was conducted through X-ray diffraction analysis (XRD) using a BRUKER D8 advance instrument. Cu K radiation (λ = 0.154 nm) was employed, with operating parameters set at 40 kV and 30 mA. The scanning of 2θ-degree patterns was performed at a rate of 5°/min within the range spanning from 5° to 80°.To identify the functional groups present in the Ti_3C_2 MXene nanoparticles, Fourier-Transform Infrared Spectroscopy (FTIR) analysis was carried out using a Perkin Elmer instrument (model L160000M). The FTIR spectra were recorded by accumulating 200 scans across a spectral wavenumber range of 500 to 4000 cm^{-1}. The elemental composition of the MXene material was determined through Energy-dispersive X-ray spectroscopy (EDX) using a Quanta 400F instrument from the United States. For a comprehensive examination of the morphology of the Ti_3C_2 MXene nanoparticles, Field Emission Scanning Electron Microscopy (FESEM) was employed. Specifically, a ZEISS SUPRA 55VP instrument was used for this purpose.

2.4 Formulation of Ti_3C_2 MXene Nanolubricant

The samples of MXene nanolubricant were prepared by dispersing 0.005wt.%, 0.01wt.%, and 0.05wt.% of the as-synthesized Ti_3C_2 MXene powders into 100 ml of outboard engine oil. To ensure the nanoparticles were uniformly dispersed and to achieve stability, the oil samples underwent a sonication process using a water bath sonicator for 30 minutes. They were homogenized at 5000 rpm for 10 minutes using a high-shear lab mixer to ensure uniform mixing and distribution of nanoparticles. Figure 2 shows the overall process of Ti_3C_2 MXene nanolubricant formulation.

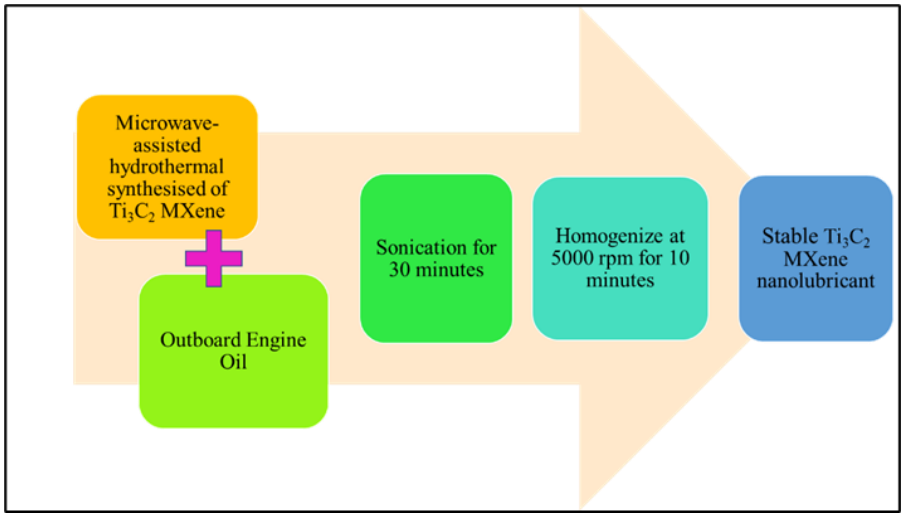

Figure 2: Process flow of Ti_3C_2 MXene nanolubricant formulation.

2.5 Formulation of Ti_3C_2 MXene Nanolubricant

In the case of each oil sample, an assessment of stability was performed through Zeta Potential analysis using the Malvern Zetasizer 3000HSA instrument. This analysis aimed to gauge the stability of the Ti_3C_2 MXene nanolubricant and to prevent the occurrence of MXene flocculation within the oil medium.

2.6 Tribotesting of Ti_3C_2 MXene Nanolubricant

The evaluation of the coefficient of friction (COF) and the average wear scar diameter (WSD) for the Ti_3C_2 MXene formulation at varying concentrations (0.05 wt%, 0.01 wt%, and 0.005 wt%), along with the base oil, was conducted using a Ducom four-ball tribometer model TR-30L. Within the tribometer, one steel ball underwent rotational motion while in contact with three additional carbon-chromium steel balls submerged in the respective nanolubricants contained within the ball pot. The physical specifications of the carbon-chromium steel balls, each having a diameter of 12.7 mm, utilized in this experimental setup are detailed in Table 1.

Table 1: The steel balls specification used in the tribometer.

Properties	Value
Material	Carbon-chromium steel
Hardness, H [HRC]	1
Density, ρ [g/cm^3]	7.79
Surface roughness, R_a [µm]	0.022

The experimental parameters adhered to the guidelines stipulated in the ASTM D 4172 standard. These parameters encompassed a rotational speed set at 1,200 revolutions per minute (rpm), an applied load of 392.5 Newtons (N), a testing duration of 3,600 seconds, and an operating temperature of 75 °C. Conforming to the ASTM D 4172 standard, these standardized conditions were employed to conduct an initial evaluation of the lubricant's anti-wear characteristics. A

detailed summary of the operational conditions for the four-ball tribotester is presented in Table 2.

Table 2: The ASTM D 4172 operating parameter for tribotesting.

Parameter	Value
Rotating speed [rpm]	1200
Appplied load [N]	392.5
Temperature [^{o}C]	75
Time [sec]	3600

The primary data processing system integrated within the tribotester was responsible for computing the coefficient of friction (COF) associated with the nanolubricant. Simultaneously, an image-capturing apparatus was employed to assess the diameter of the wear scar resulting from the tribological contact. This assessment focused on the worn scar dimensions on the stationary metal balls, serving to gauge the extent of wear. Throughout the tribotesting, stringent temperature control was maintained, with the lubricant environment consistently held at a stable temperature of 75 °C. To cleanse the steel balls post-test, ethanol was utilized as the cleaning agent. Additionally, an optical microscope was deployed to conduct a detailed examination of the weathered scar surfaces.

2.7 Thermal Conductivity Evaluation of Ti_3C_2 MXene Nanolubricant

With the aid of the LFA HyperFlash device from NETZSCH, Germany, the thermal conductivity of lubricating oil samples containing various Ti_3C_2 MXene concentrations was assessed using laser flash analysis (LFA). The experiment was conducted in a nitrogen-filled environment. Before fitting the sample holder components together, the cover of the lubricating oil samples was coated with graphite to aid in heat absorption. The samples were heated up gradually for the LFA analysis.

3.0 RESULTS AND DISCUSSION

3.1 Characterization of Ti_3C_2 MXene Nanoparticles

Figure 3 presents a comprehensive set of characterization results for both the bulk MAX phase precursor and the as-synthesized Ti_3C_2 MXene. These results assess their phase structure, crystallinity, morphology, elemental composition, and functional groups. Regarding the X-ray diffraction (XRD) analysis, as depicted in Figure 3(a), it substantiates the successful conversion of MAX phase Ti_3AlC_2 into Ti_3C_2 MXene through advanced microwave-assisted hydrothermal synthesis involving etching and exfoliation processes. In the XRD data, discernible diffraction peaks associated with distinct crystallographic planes are observed for the MAX phase, including (002), (004), (101), (103), (104), (105), (109), and (110), situated at respective angles of 9.7°, 19.2°, 34.1°, 39.0°, 41.9°, 56.5°, and 60.4°. These observations are in agreement with established standard values (JCPDS No. 52-0875). Following the advanced microwave-hydrothermal synthesis, the previously sharp peaks corresponding to Ti_3AlC_2 undergo a significant reduction in intensity. Notably, the (002) diffraction peak experiences a distinct shift, transitioning from 9.64° to 6.13° and 6.54° for Ti_3C_2 MXene, signifying notable changes in grain size and interlayer spacing within the Ti_3C_2 sample.

Figure 3(b) demonstrates the Fourier-Transform Infrared Spectroscopy (FTIR) results. This analysis offers insights into the chemical bonding of the MAX phase, surface termination groups, and the delaminated Ti_3C_2 MXene. Comparable stretching vibrations are observed in both the MAX phase and MXene, encompassing Ti-C, Ti-O, C-O, and C-C vibrations. Additionally, hydrogen bonding is discerned in both samples. The FTIR spectra further reveal the presence of distinct vibrational modes associated with Ti-O, Ti-C, CO, OH, -Ox, and C-F groups, aligning with previous research findings (He et al., 2022; Z. Liu et al., 2022), indicating a variety of surface terminations in the MXene prepared through the microwave-assisted hydrothermal method.

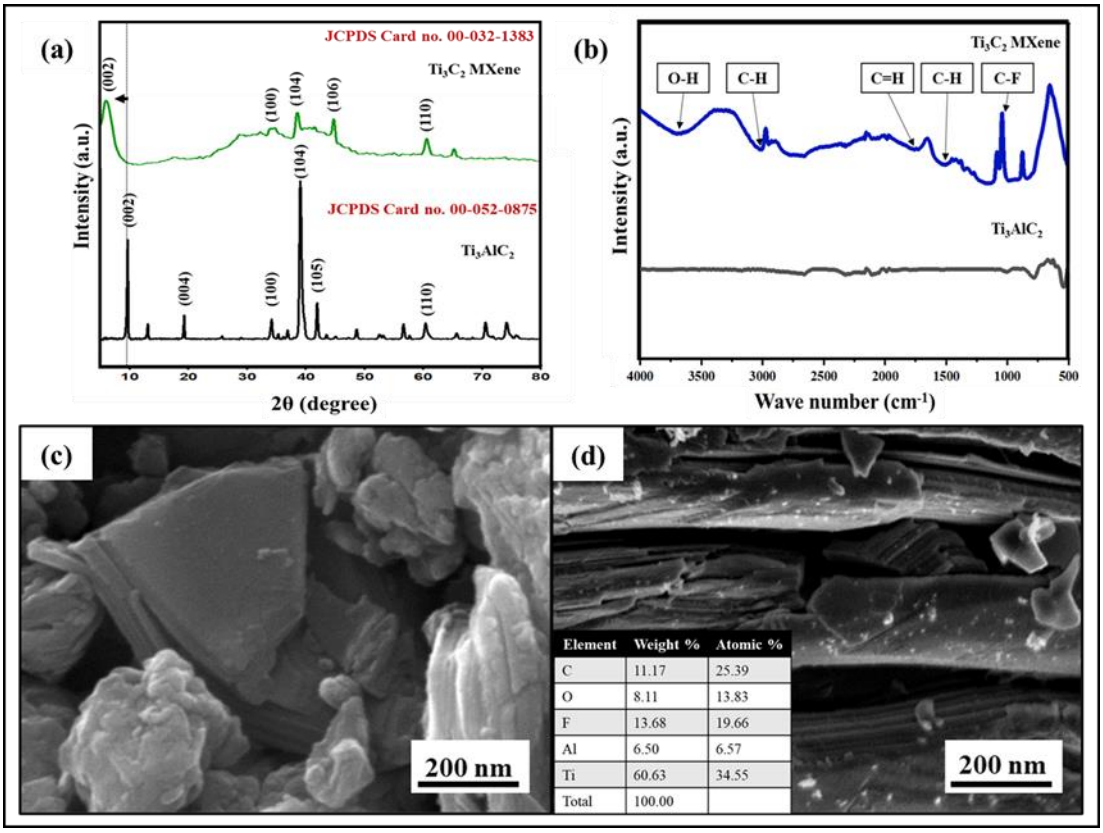

Figure 3: (a) XRD diffractogram of MAX phase and Ti_3C_2 MXene, (b) FTIR of MAX phase and Ti_3C_2 MXene, (c) FESEM micrograph of MAX phase and (d) FESEM and EDX of Ti_3C_2 MXene.

The FESEM images in Figure 3 (c) and (d) revealed the morphological changes after etching and exfoliation. The MAX phase Ti_3AlC_2 exhibited a solid, stacked multilayer nanosheet structure (**Error! Reference source not found.** 3(c)). In contrast, the MXene samples (Figure 3 (d)) showed individual layers of MXene sheets with nanosheets size around 12 nm, indicating that Al had been removed from the MAX layers. This showed that the microwave-assisted hydrothermal technique effectively produced thin layers of 2D MXene nanosheets. EDX elemental spectrum in Figure 3 (d) confirmed the existence of Ti, C, F, and a negligible amount of Al in both MXene samples. This analysis verified the establishment of MXene and removed a large amount of Al elements from the precursor. The characterization studies confirmed the establishment of Ti_3C_2

MXene from its precursor, the morphological changes after etching and exfoliation, and the presence of several surface termination groups in the synthesized MXene.

3.2 Zeta potential of Ti_3C_2 MXene Nanolubricant

Figure 4 displays the zeta potential of Ti_3C_2 MXene nanolubricant prior to and after 14 days. The zeta potential measurements indicate that the MXene nanolubricant formulation exhibits excellent stability, with zeta potential values exceeding 61 mV. This stability is observed both before and after the 14-day interval. However, it is noted that the stability of the MXene nanolubricant gradually decreases after 14 days, indicating the occurrence of slow coagulation of MXene nanoparticles. Additionally, a linear decrease in the zeta potential value is observed with increasing Ti_3C_2 MXene concentration. This implies that the mobility of nanoparticles is constrained at larger concentrations, impeding the development of an energy barrier and leading to particle aggregation and precipitation. In other contexts, the repelling forces between nanoparticles weaken at exceeding concentrations, causing them to accumulate and have a lower zeta potential value.

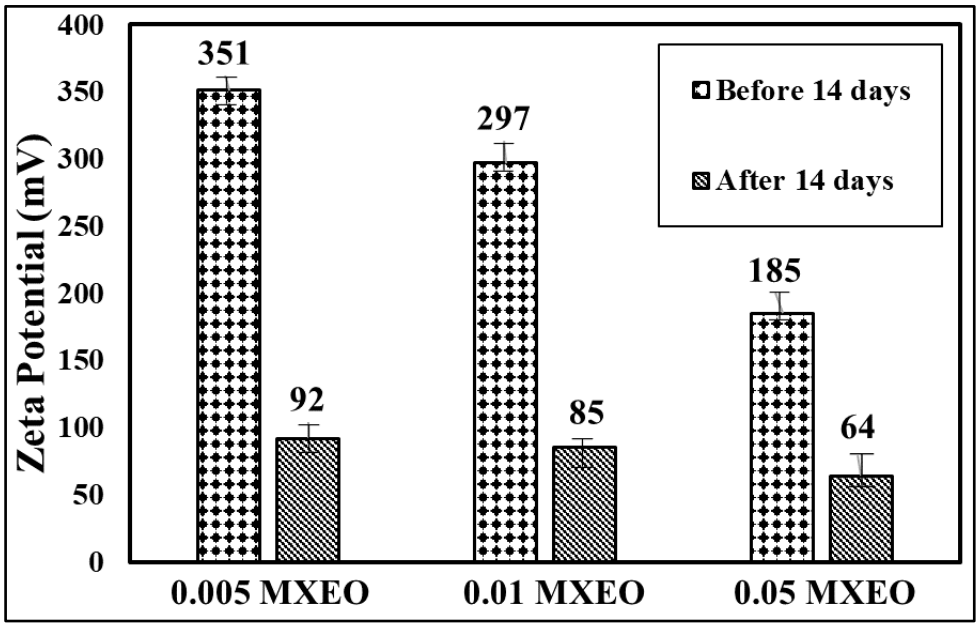

Figure 4: Zeta potential size of the Ti_3C_2 MXene nanolubricant with various concentrations.

3.3 Tribological analysis of Ti_3C_2 MXene Nanolubricant

The influence of nano-additives on the performance of lubricating oil has been scrutinized, with notable findings reported by (Zaharin et al., 2023). Figure 5 illustrates the outcomes in terms of the coefficient of friction (COF) and the wear scar diameter (WSD) for MXene nanolubricants containing varying concentrations of Ti_3C_2 MXene nanoparticles within outboard engine oil.In Figure 5(a), the COF of the base oil registers at 0.1252. Upon introducing 0.01 wt.% of MXene into the base oil, an initial reduction in COF is observed. This decrease is attributed to the formation of a protective shielding layer comprising MXene nanosheets within the lubricant. This layer effectively mitigates friction by impeding the slippage of individual layers. As the MXene

nanolayers reach a sufficient concentration, they contribute to the formation of a uniform tribofilm during sliding and deformation, thus further diminishing friction. However, when the concentration reaches 0.05 wt.%, a noteworthy increase in COF occurs. This phenomenon indicates the aggregation of Ti_3C_2 MXene nanoparticles, resulting in flocculation. Consequently, the nanoparticles face hindrances in accessing the minute gaps between the frictional contact points, leading to an elevated COF. This trend is consistent with observations made by (Guo et al., 2022; Nagarajan et al., 2022).

Figure 5(b) illustrates the WSD for outboard engine oil with varying levels of MXene additives. The base oil yields a WSD of 818 µm. Incorporating Ti_3C_2 MXene additives ranging from 0.005 wt.% to 0.05 wt.% in the oil leads to a notable enhancement in WSD, with improvements ranging from 3.0% to 8.2% compared to the base oil. The most favourable outcome is achieved with 0.01 wt.% Ti_3C_2 MXene additive. This outcome aligns with research conducted by Markandan et al. and other researchers (Markandan et al., 2023; Mushtaq & Hanief, 2021), which highlights that the creation of a thin lubricating layer sandwiched between interacting surfaces results in a reduction in WSD.

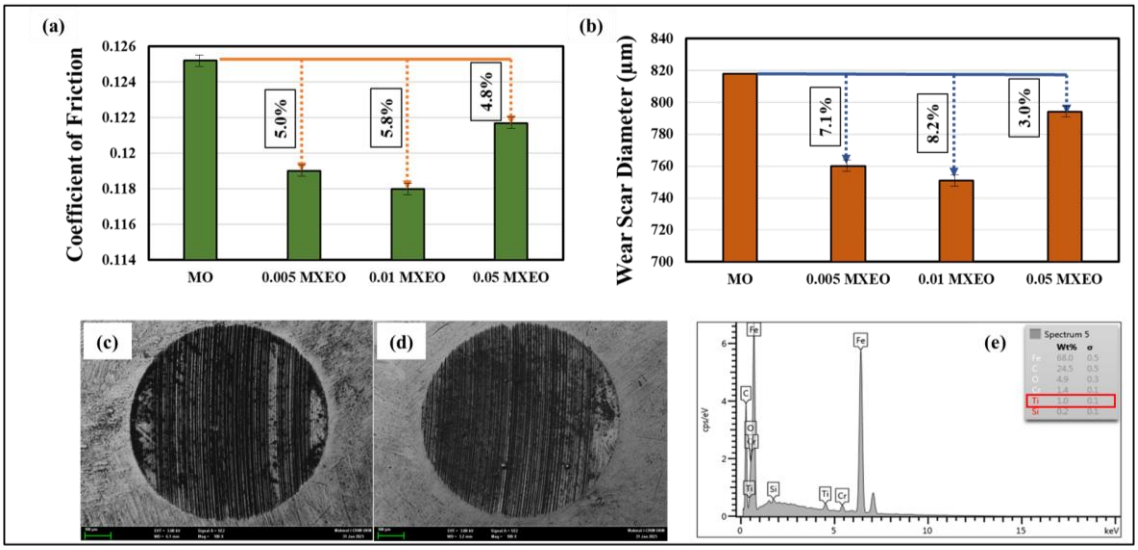

Figure 5: (a) COF of MXEO with different concentrations, (b) WSD of MXEO with different concentrations. FESEM images of the wear scar of the ball with (c) base oil and (d) 0.01 wt.% MXEO. (d) EDX elemental spectrum of wear scar of the ball with 0.01 wt.% MXEO.

This layer not only mitigates frictional torque and contact pressure but also facilitates the accumulation and deposition of nanoparticles within microscopic fissures and ridges, thereby smoothening the surfaces and reducing the average WSD. This phenomenon underscores an additional mechanism contributing to the beneficial mending effect.

The results obtained from Field Emission Scanning Electron Microscopy (FESEM) and Energy-Dispersive X-ray Spectroscopy (EDX) analyses, as depicted in Figure 5(c) through (e), serve to corroborate the preceding observations. In particular, these analyses provide empirical support for the identified surface wear and composition trends.

Figure 5(c) and (d) reveal significant disparities in the surface characteristics of the ball bearing subjected to base oil versus the ball bearing augmented with 0.01 wt.% Ti_3C_2 MXene additive. The

former exhibits pronounced furrows and deeper surface abrasions, indicating increased wear and friction. In contrast, the addition of 0.01 wt.% Ti_3C_2 MXene results in shallower furrows and conspicuously smooth wear tracks. This outcome underscores the ability of MXene nanolayers to swiftly traverse the oil surface, thereby generating a continuous protective coating on the sliding surfaces. This coating, characterized by excellent contact adhesion, aligns with earlier research findings (Zaharin et al., 2023; Zhang et al., 2019). This mending property is instrumental in repairing scratched and worn surfaces, establishing a protective layer, and minimising direct surface-to-surface contact, consequently reducing wear scar diameter. Notably, the presence of titanium, as evidenced by the EDX analysis, confirms the adherence of Ti_3C_2 MXene nanoparticles within surface cracks, resulting in a reduction in groove depth. The introduction of Ti_3C_2 into the lubricating oil yields enhanced tribological properties, attributable to the development of a tribofilm and the associated mending effect. Thanks to its two-dimensional structure, Ti_3C_2 MXene exhibits a propensity to traverse the oil surface readily. However, it is imperative to acknowledge that as the concentration of Ti_3C_2 MXene increases, aggregation tendencies become more prominent, engendering heightened tribological effects between mating surfaces. These findings remain consistent with prior studies that have demonstrated a significant reduction in the coefficient of friction (COF) and wear characteristics when Ti_3C_2 MXene is harnessed as a nanolubricant, as documented in the works of (L. Liu et al., 2019; Suresha et al., 2019; Zaharin et al., 2023).

3.4 Thermal Analysis of Ti_3C_2 MXene Nanolubricant

Elevated thermal conductivity in lubricants is imperative for effectively mitigating engine heat and mechanical fatigue. The analysis of thermal conductivity was undertaken on Ti_3C_2 MXene nanolubricant samples blended with TC-W-qualified outboard engine oil. This analysis encompassed variations in concentration and temperature, spanning the range of 40°C to 100°C.

The findings unveiled a direct relationship between the concentration of Ti_3C_2 MXene nanoparticles and the thermal conductivity of the nanolubricant. Notably, as the concentration of MXene nanoparticles in the oil sample increased, the thermal conductivity exhibited a corresponding enhancement. The rationale behind this phenomenon lies in the augmented dispersion of higher MXene concentrations, which facilitates superior heat dissipation and intensified molecular collisions within the lubricant. Consequently, this augmentation culminates in elevated thermal conductivity. Notably, Figure 6 illustrates that the highest concentration of MXene nanolubricant, denoted as 0.05 MXEO, yields the most pronounced increase in thermal conductivity. This can be attributed to the distinctive high aspect ratio and layered morphology of Ti_3C_2 MXene nanosheets, which effectively engender a more extensive contact interface, thereby contributing to the observed elevation in thermal conductivity.

Moreover, it was observed that thermal conductivity exhibited an upward trend with increasing temperature within the range of 40°C to 100°C. This can be ascribed to the heightened molecular vibrations and random collisions that occur at elevated temperatures. At lower temperatures, the lubricant's elevated viscosity imposes constraints on the mobility of Ti_3C_2 MXene nanosheets, consequently diminishing thermal conductivity. However, as temperature increases, the reduction in viscosity facilitates greater mobility of these nanosheets, thereby fostering enhanced Brownian motion and resulting in a more pronounced thermal conductivity. This phenomenon aligns with prior studies, which have underscored the relationship between rising temperature, decreasing viscosity, heightened mobility, and improved thermal conductivity.(Apmann et al., 2021; Malekzadeh et al., 2016).

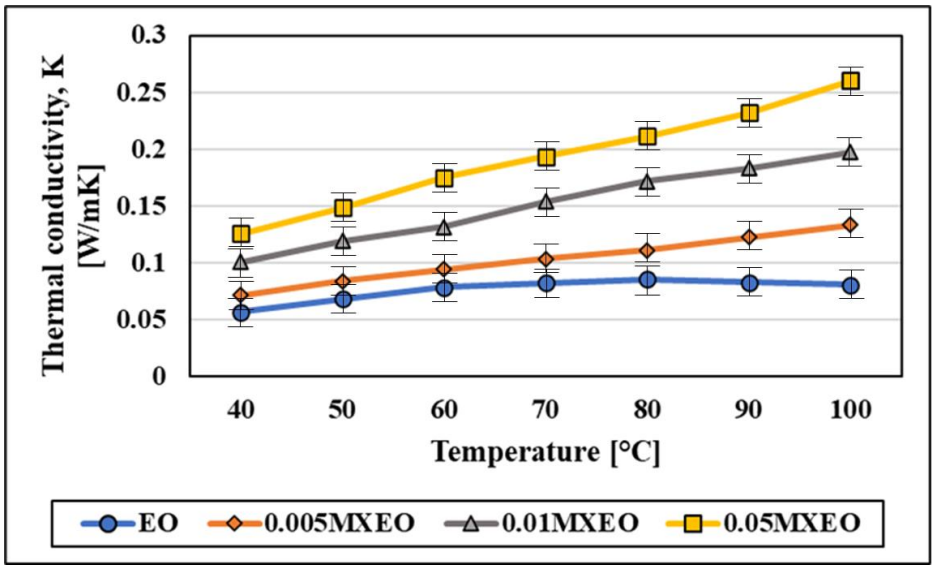

Figure 6: Thermal conductivity of Ti_3C_2 MXene nanolubricant with various concentration.

3.5 Lubricating Mechanism of Ti_3C_2 MXene Additive

The realm of tribology, concerned with understanding and reducing friction and wear between interacting surfaces, has witnessed a transformative shift with the advent of advanced nanomaterials. Among these, Ti_3C_2 MXene nanoparticles have emerged as promising additives in nanolubricants, potentially enhancing lubrication performance significantly.

At the heart of the lubricating mechanism lies the ability of Ti_3C_2 MXene nanoparticles to adhere to and form a shielding layer on the contacting interfaces. These nanoparticles possess a high surface area and unique surface chemistry, facilitating strong adhesion to metal surfaces. These nanoparticles easily migrate to the asperities and micro-gaps on the contact areas when exposed to the nanolubricant, forming a strong boundary lubrication zone. This layer lowers friction and wear by eliminating immediate contact between the two surfaces by serving as a barrier.

As the Ti_3C_2 MXene nanoparticles form a boundary lubrication layer, they undergo a process of tribofilm formation. Under mechanical and thermal forces, these nanoparticles interact with the lubricant's base oil and undergo chemical transformations, generating a complex tribochemical film on the surfaces. This tribofilm serves multiple purposes: it reduces wear by sacrificially abrading during sliding, provides a smooth sliding interface, and absorbs energy through its deformation, thereby cushioning impacts between the surfaces.

One of the remarkable traits of Ti_3C_2 MXene nanoparticles is their shear stability within the lubricant film. Due to their nanoscale dimensions and inherent mechanical robustness, these particles withstand shear forces without undergoing excessive deformation. This characteristic ensures the longevity of the boundary lubrication layer, sustaining its effectiveness even under high-stress conditions. Furthermore, the nanoparticles can distribute mechanical loads across the surfaces, enhancing load-bearing capacity and minimizing surface deformation and wear.

In addition, nanolubricants containing Ti_3C_2 MXene nanoparticles also benefit from these additives' thermal conductivity enhancement properties. The high thermal conductivity of MXene

materials facilitates efficient heat dissipation from the frictional zone, lowering the possibility of thermal deterioration and keeping the lubricant's performance stable under elevated temperatures. This property is particularly advantageous in high-performance engines where heat generation is significant.

Overall, the lubricating mechanism of Ti_3C_2 MXene additives in nanolubricants is a complex interplay of surface adhesion, tribofilm formation, shear stability, load-bearing capacity, and thermal conductivity enhancement. These nanoparticles offer a multifaceted approach to reducing friction and wear by forming a protective boundary layer, absorbing energy, and enhancing thermal management. As research unravels these interactions' intricacies, the potential for tailoring and optimizing the lubricating mechanism becomes increasingly promising. Adopting Ti_3C_2 MXene additives in nanolubricants holds great potential to revolutionize tribological practices across industries, paving the way for more efficient and durable machinery and reducing environmental impact.

ACKNOWLEDGEMENT

The authors gratefully acknowledge the Ministry of Higher Education Malaysia and Universiti Kebangsaan Malaysia (grant number FRGS/1/ 2018/TK03/UKM/02/8).

CONCLUSIONS

In summary, the optimal concentration of Ti_3C_2 MXene nanoparticles in the nanolubricant, specifically at 0.01 wt.%, yielded the most favourable outcomes in this study. Comparative analysis with the base oil revealed a notable reduction of 5.8% in the coefficient of friction (COF) and an 8.2% decrease in the average wear scar diameter (WSD). These improvements can be ascribed to the formation of a protective film known as the tribofilm, which effectively develops between the surfaces undergoing friction, thereby significantly diminishing the friction coefficient. Furthermore, the reduction in wear scar diameter can be attributed to a repairing effect, where Ti_3C_2 MXene nanoparticles congregate and seal surface cracks and crevices, thereby preventing direct contact and reducing wear. Additionally, the incorporation of MXene nanoparticles yielded a positive trend in thermal conductivity, resulting in a substantial improvement of over 50% compared to the base oil. This enhancement can be attributed to several contributing factors, including the high aspect ratio of the nanoparticles, their layered morphology, and the Brownian motion they induce, collectively augmenting the overall thermal conductivity of the nanolubricant.In summary, the comprehensive test results affirm a nanolubricant comprising 0.01 wt.% MXene nanoparticles exhibited the most substantial enhancements in both tribological performance and thermal conductivity analyses.

REFERENCES

Al-Janabi, A. S., Hussin, M., & Abdullah, M. Z. (2021). Stability, thermal conductivity and rheological properties of graphene and MWCNT in nanolubricant using additive surfactants. Case Studies in Thermal Engineering, 28(October), 101607. https://doi.org/10.1016/j.csite.2021.101607

Anasori, B., Lukatskaya, M. R., & Gogotsi, Y. (2017). 2D metal carbides and nitrides (MXenes) for energy storage. Nature Reviews Materials, 2(2). https://doi.org/10.1038/natrevmats.2016.98

Apmann, K., Fulmer, R., Soto, A., & Vafaei, S. (2021). Thermal Conductivity and Viscosity: Review

and Optimization of Effects of Nanoparticles. Materials, 14(5), 1291. https://doi.org/10.3390/ma14051291

Cai, M., Feng, P., Yan, H., Li, Y., Song, S., Li, W., Li, H., Fan, X., & Zhu, M. (2022). Hierarchical Ti3C2T@MoS2 heterostructures: A first principles calculation and application in corrosion/wear protection. Journal of Materials Science & Technology, 116, 151–160. https://doi.org/10.1016/j.jmst.2021.11.026

Guo, J., Wu, P., Zeng, C., Wu, W., Zhao, X., Liu, G., Zhou, F., & Liu, W. (2022). Fluoropolymer grafted Ti3C2Tx MXene as an efficient lubricant additive for fluorine-containing lubricating oil. Tribology International, 170, 107500. https://doi.org/10.1016/j.triboint.2022.107500

Gupta, D., Chauhan, V., & Kumar, R. (2020). A comprehensive review on synthesis and applications of molybdenum disulfide (MoS2) material: Past and recent developments. In Inorganic Chemistry Communications (Vol. 121). Elsevier B.V. https://doi.org/10.1016/j.inoche.2020.108200

He, X., Li, S., Shen, R., Ma, Y., Zhang, L., Sheng, X., Chen, Y., Xie, D., & Huang, J. (2022). A high-performance waterborne polymeric composite coating with long-term anti-corrosive property based on phosphorylation of chitosan-functionalized Ti3C2Tx MXene. Advanced Composites and Hybrid Materials, 5(3), 1699–1711. https://doi.org/10.1007/s42114-021-00392-0

Ji, Z., Zhang, L., Xie, G., Xu, W., Guo, D., Luo, J., & Prakash, B. (2020). Mechanical and tribological properties of nanocomposites incorporated with two-dimensional materials. Friction, 8(5), 813–846. https://doi.org/10.1007/s40544-020-0401-4

Liu, L., Zhou, M., Jin, L., Li, L., Mo, Y., Su, G., Li, X., Zhu, H., & Tian, Y. (2019). Recent advances in friction and lubrication of graphene and other 2D materials: Mechanisms and applications. Friction, 7(3), 199–216. https://doi.org/10.1007/s40544-019-0268-4

Liu, Y. (2016). Synthesis and tribological property of Ti 3 C 2 T X nanosheets. Journal of Materials Science. https://doi.org/10.1007/s10853-016-0509-0

Liu, Z., Lv, H., Xie, Y., Wang, J., Fan, J., Sun, B., Jiang, L., Zhang, Y., Wang, R., & Shi, K. (2022). A 2D/2D/2D Ti 3 C 2 T x @TiO 2 @MoS 2 heterostructure as an ultrafast and high-sensitivity NO 2 gas sensor at room-temperature. Journal of Materials Chemistry A, 10(22), 11980–11989. https://doi.org/10.1039/D1TA09369J

Malekzadeh, A., Pouranfard, A. R., Hatami, N., Kazemnejad Banari, A., & Rahimi, M. R. (2016). Experimental Investigations on the Viscosity of Magnetic Nanofluids under the Influence of Temperature, Volume Fractions of Nanoparticles and External Magnetic Field. Journal of Applied Fluid Mechanics, 9(2), 693–697. https://doi.org/10.18869/acadpub.jafm.68.225.24022

Manu, B. R., Gupta, A., & Jayatissa, A. H. (2021). Tribological properties of 2D materials and composites- A review of recent advances. Materials, 14(7). https://doi.org/10.3390/ma14071630

Markandan, K., Nagarajan, T., Walvekar, R., Chaudhary, V., & Khalid, M. (2023). Enhanced Tribological Behaviour of Hybrid MoS2@Ti3C2 MXene as an Effective Anti-Friction Additive in Gasoline Engine Oil. Lubricants, 11(2). https://doi.org/10.3390/lubricants11020047

Masjuki, H. H., Kalam, M. A., & Yunus, R. (2014). Lubricity of bio-based lubricant derived from chemically modified jatropha methyl ester Corresponding author : nurinmz@um.edu.my Dimensionless minimum film thickness Dynamic viscosity at atmospheric pressure Rotational ball Stationary ball Modulus elastic. Jurnal Tribologi, 1(May), 18–39.

Mushtaq, Z., & Hanief, M. (2021). Enhancing the tribological characteristics of Jatropha oil using graphene nanoflakes. Jurnal Tribologi, 28(February), 129–143.

Nagarajan, T., Khalid, M., Sridewi, N., Jagadish, P., Shahabuddin, S., Muthoosamy, K., & Walvekar, R. (2022). Tribological, oxidation and thermal conductivity studies of microwave synthesized molybdenum disulfide (MoS2) nanoparticles as nano-additives in diesel based engine oil. Scientific Reports, 12(1), 14108. https://doi.org/10.1038/s41598-022-16026-4

Naguib, M., Mochalin, V. N., Barsoum, M. W., & Gogotsi, Y. (2013). 25th Anniversary Article : MXenes : A New Family of Two-Dimensional Materials. 992–1005. https://doi.org/10.1002/adma.201304138

Nasrallah, G. K., Al-Asmakh, M., Rasool, K., & Mahmoud, K. A. (2018). Ecotoxicological assessment of Ti 3 C 2 T x (MXene) using a zebrafish embryo model. Environmental Science: Nano, 5(4), 1002–1011. https://doi.org/10.1039/C7EN01239J

Numan, A., Rafique, S., Khalid, M., Zaharin, H. A., Radwan, A., Mokri, N. A., Ching, O. P., & Walvekar, R. (2022). Microwave-assisted rapid MAX phase etching and delamination: A paradigm shift in MXene synthesis. Materials Chemistry and Physics, 288, 126429. https://doi.org/10.1016/j.matchemphys.2022.126429

Pan, S., Yin, J., Yu, L., Zhang, C., Zhu, Y., Gao, Y., & Chen, Y. (2020). 2D MXene-Integrated 3D-Printing Scaffolds for Augmented Osteosarcoma Phototherapy and Accelerated Tissue Reconstruction. Advanced Science, 7(2), 1901511. https://doi.org/10.1002/advs.201901511

Rahman, N. L., Amiruddin, H., Abdollah, M. F. B., Umehara, N., & Tunggal, D. (2023). Synthesis and characterisation of oil palm fibre-based graphene deposited on copper particles for superlubricity oil additive. Jurnal Tribologi, 37, 128-141.

Rasheed, A. K., Khalid, M., Mohd Nor, A. F. Bin, Wong, W. Y., Duolikun, T., Natu, V., Barsoum, M. W., Leo, B. F., Zaharin, H. A., & Ghazali, M. J. (2020). MXene-graphene hybrid nanoflakes as friction modifiers for outboard engine oil. IOP Conference Series: Materials Science and Engineering, 834(1). https://doi.org/10.1088/1757-899X/834/1/012039

Rosenkranz, A., Grützmacher, P. G., Espinoza, R., Fuenzalida, V. M., Blanco, E., Escalona, N., Gracia, F. J., Villarroel, R., Guo, L., Kang, R., Mücklich, F., Suarez, S., & Zhang, Z. (2019). Multi-layer Ti3C2Tx-nanoparticles (MXenes) as solid lubricants – Role of surface terminations and intercalated water. Applied Surface Science, 494(April), 13–21. https://doi.org/10.1016/j.apsusc.2019.07.171

Rosenkranz, A., Liu, Y., Yang, L., & Chen, L. (2020). 2D nano-materials beyond graphene: from synthesis to tribological studies. In Applied Nanoscience (Switzerland) (Vol. 10, Issue 9). Springer International Publishing. https://doi.org/10.1007/s13204-020-01466-z

Rosenkranz, A., Righi, M. C., Sumant, A. V., Anasori, B., & Mochalin, V. N. (2023). Perspectives of 2D MXene Tribology. Advanced Materials, 35(5), 2207757. https://doi.org/10.1002/adma.202207757

Shahdeo, D., Roberts, A., Abbineni, N., & Gandhi, S. (2020). Graphene based sensors. In Comprehensive Analytical Chemistry (1st ed., Vol. 91). Elsevier B.V. https://doi.org/10.1016/bs.coac.2020.08.007

Suresha, B., Hemanth, G., Rakesh, A., & Adarsh, K. M. (2019). Tribological behaviour of pongamia oil as lubricant with and without halloysite nanotubes using four-ball tester. 030011. https://doi.org/10.1063/1.5117954

Verger, L., Natu, V., Carey, M., & Barsoum, M. W. (2019). MXenes: An Introduction of Their Synthesis, Select Properties, and Applications. Trends in Chemistry, 1(7), 656–669. https://doi.org/10.1016/j.trechm.2019.04.006

Yang, L., Mao, M., Huang, J. nan, & Ji, W. (2019). Enhancing the thermal conductivity of SAE 50 engine oil by adding zinc oxide nano-powder: An experimental study. Powder Technology, 356,

335–341. https://doi.org/10.1016/j.powtec.2019.08.031
Ying, Y., Liu, Y., Wang, X., Mao, Y., Cao, W., Hu, P., & Peng, X. (2015). Two-dimensional titanium carbide for efficiently reductive removal of highly toxic chromium(VI) from water. ACS Applied Materials and Interfaces, 7(3), 1795–1803. https://doi.org/10.1021/am5074722
Zaharin, H. A., Ghazali, M. J., Khalid, M., Nagarajan, T., Pin, W. W., Ezzah, F., Gerard, O., Walvekar, R., & Rasheed, A. K. (2023). Tribological, Oxidation and Thermal Analysis of Advanced Microwave–Hydrothermal Synthesised Ti3C2Tx MXene as Additives in Outboard Engine Oil. Lubricants, 11(6), 264. https://doi.org/10.3390/lubricants11060264
Zaharin, H. A., Ghazali, M. J., Numan, A., Khalid, M., Thachnatharen, N., Ezzah, F., & Rasheed, A. K. (2023). Tribological Investigation of 2D Ti3C2 MXene Via Microwave-Assisted Hydrothermal Synthesis as Additives for Different Lubrications (pp. 775–782). https://doi.org/10.1007/978-981-19-9267-4_76
Zaharin, H. A., Ghazali, M. J., Rasheed, A. K., Khalid, M., & Otsuka, Y. (2022). Tribological Performance of Hybrid Ti3C2/Graphene Additive on Outboard Engine Oil. In Proceedings of the Malaysian International Tribology Conference (pp. 146–153). https://doi.org/10.1007/978-981-16-9949-8_29
Zaharin, H. A., Ghazali, M. J., Thachnatharen, N., Ezzah, F., Walvekar, R., & Khalid, M. (2023). Progress in 2D materials based Nanolubricants: A review. FlatChem, 38(January), 100485. https://doi.org/10.1016/j.flatc.2023.100485
Zhang, X., Guo, Y., Li, Y., Liu, Y., & Dong, S. (2019). Preparation and tribological properties of potassium titanate-Ti3C2Tx nanocomposites as additives in base oil. Chinese Chemical Letters, 30(2), 502–504. https://doi.org/10.1016/j.cclet.2018.07.007